Spontaneous passivation observations during scale formation on mild steel in CO₂ brines☆

Jiabin Han *, Srdjan Nešić **, Yang Yang, Bruce N. Brown

Institute for Corrosion and Multiphase Technology, Department of Chemical and Biomolecular Engineering, Ohio University, 342 West State Street, Athens, OH 45701, United States

ABSTRACT

Previous study revealed localized corrosion in CO_2 environments was driven by a galvanic cell established between pit surfaces and scaled surrounding area. In order to underpin the understanding of the galvanic mechanism of localized corrosion, the root cause of potential differences between these two surfaces, passivation of mild steel, in CO_2 environments was investigated using transmission electron microscopy technique and electrochemical techniques including potentiodynamic polarization, cyclic polarization and open circuit potential techniques. Potentiodynamic polarization experiments showed that the passivation of the carbon steel surface favorably occurred at pH > 7 and facilitated with the presence of $FeCO_3$ scale. Cyclic polarization tests showed that polarization rate had an important influence on passivation behavior. At a slower polarization rate, lower passivation potential and current density were observed. Spontaneous passivation was evidenced by a significant increase of corrosion resistance and an open circuit potential without any externally applied current or potential during electrode immersion. This process is affected by pH, temperature, presence of CO_2 and iron carbonate. Nevertheless, iron carbonate film is not the only one responsible for passivation, as demonstrated from depassivation tests where passivity was lost without losing the existing iron carbonate film. Transmission electron microscopy technique was used to determine the structure of the passive layer. An extra phase, most likely magnetite, was observed to be beneath the iron carbonate scale and at the crystal grain boundaries which passivated the mild steel.

© 2011 Elsevier Ltd. All rights reserved.

1. Introduction

Corrosion costs more than 3% of US GDP according to a survey conducted in 2002 [1] and 90% of failures are caused by localized corrosion [2], in which the material corrodes in small regions at rates tens, even hundreds of times faster than uniform/general corrosion. This subject has been of much interest for several decades. Many researchers and scientists have put much effort to explore this problem [3–22]. Most of previous researches on localized corrosion have focused on passive metals, which include stainless steel, aluminum, molybdenum, nickel, etc, as well as carbon steel under some conditions. Classically, passivation can generally be distinguished by electrochemical definitions that "the metal substantially resists corrosion in a given environment despite a

marked thermodynamic tendency to react" (e.g. high corrosion resistivity at relatively high potentials) [23]. Usually, passivated metals are protected by a very thin (nanometer level) but compact oxide/hydroxide film with little porosity. These films are formed spontaneously and instantly comparing to scale formation in CO_2 brine which takes hours and days [24]. However, the stability of these films are affected by many factors including metallurgical (alloy composition [8], inclusions [9], etc.), environmental (pH [10], cations and anions [7], deposits [11], fluid dynamics [12], etc.) and mechanical (structure [13], defects [18–20], etc.). Damage of the passive films may result in severe localized corrosion. Many theoritical and mechanistic models were developed to predict formation and breakdown of the passive films accounting above factors [18–22]. Carefully analyzing the previous research with respect to the experimental methods, most of them were carried out by potentiodynamic/galvanostatic polarization, applying potential/current on metal surface to artificially passivate, de-passivate and repassivate metals.

The mechanism of localized corrosion in CO_2 envrionments has been explored since the initial uniform CO_2 corroison mehcnaism was reported in 1970 [25]. Localized corrosion can damage infrastructure walls to the point of failure within months, at rates that can be magnitudes higher than that observed for uniform/general

---

corrosion. Catastrophic failures were reported frequently due to localized CO_2 corrosion in internal pipeline corrosion in oil and gas transmission systems [26,27]. Developing theories that underpin the understanding localized CO_2 corrosion mechanism is of central importance [28–50]. Nyborg and Dugstad used an optical imaging technique and found severe localized CO_2 corrosion was initiated due to local damage to a protective $FeCO_3$ corrosion product film [30,31]. However, some fundamental questions of localized corrosion remain open:

- Why is the localized corrosion rate much higher than the uniform corrosion rate on bare metal surfaces under the same bulk conditions?
- Which conditions result in continuous propagation of localized CO_2 corrosion?

Han et al. studied localized corrosion of mild steel in near-neutral (pH) CO_2 brines using an artificial pit technique [45–50] which was successfully applied in related fields [42–44,51,52]. They established a galvanic mechanism for localized CO_2 corrosion propagation (Fig. 1). Han observed that a galvanic cell was established between the pit area (usually bare-exposed to the corrosive environment) and the surrounding surface (covered by a corrosion scale). Electrochemical measurements showed that the open circuit potentials (OCP) of the two surfaces were different: the OCP on the scaled surface (serving as cathode) was higher than that of the bare surface in a pit (anode). Thus, the bare pit anode was polarized positively by the scaled cathode while the cathode was polarized negatively by the anode to the equilibrium potential (mixed potential or coupled potential). The contribution from the cathode was dominant because the ratio of cathode area to anode area was large, i.e., approximately 1000 in the artificial pit. As a result, the anode was corroded much faster due to being positively polarized. This galvanic couple drove localized corrosion. A steady galvanic current, or continuous localized corrosion propagation, was typically observed near the saturation point with respect to iron carbonate. Therefore, the questions posed above can be explicitly answered respectively:

○ Galvanic effect: the potential of the cathode (scale covered surface) is more positive than that of the anode (bare pit surface). As a result, the anodic iron dissolution reaction is accelerated as it is polarized positively by the cathode of the galvanic cell.
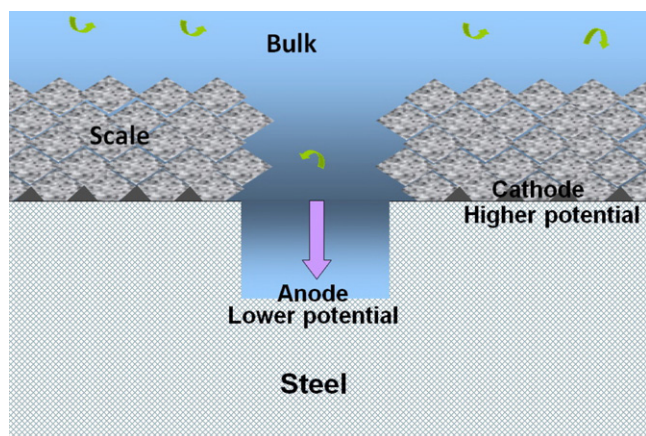○ Localized corrosion propagates steadily when the solution is near saturation point with respect to $FeCO_3$.

Fig. 1. Scheme for 1-D galvanic mechanism of localized CO_2 corrosion on mild steel.

The critical gap in the theory of the galvanic mechanism is: why the scaled surface developed a higher potential compared with the bare steel surface. A number of scenarios can be examined. If the transfer of a reactant for the cathodic reaction was retarded by the corrosion scale, cathodic current becomes diffusion limited while the anodic reaction remains under activation reaction control, i.e., iron dissolution. Then the open circuit potential decreases with scale formation compared with that of the bare surface [53]. However, this was found to be the case only in the beginning of the process of iron carbonate scale formation but ultimately the opposite happened: the potential increased as presented in experimental results section below.

On the other hand, if we assume that the corrosion process remains under electrochemical charge transfer control (activation control) and both the anodic and cathodic reactions are proportionally retarded due to scale formation, the open circuit potential would remain approximately the same) [53]. This was not the case and this scenario can be discarded.

If charge transfer control of the electrochemical reactions persists during scale formation but somehow the cathodic reactions are reduced more than the anodic reactions, the open circuit potential decreases under scaling conditions [53]. Nevertheless, it is now much harder to explain why this selective retardation of the cathodic charge transfer would occur by inert and nonconductive $FeCO_3$.

In another possible situation, both reactions remain under charge transfer control but the anodic reaction is selectively more retarded under scale forming conditions. The open circuit potential increases under scaling conditions compared with non-scaling conditions [53]. This is a plausible scenario, given the observed behavior, but it remains hard to explain why this selective retardation occurs.

One possibility includes steel surface passivation. This offers an explanation why the open circuit potential increases after scale formation. This could be due to formation of a thin but protective layer that slows down anodic dissolution of iron (akin to what occurs for stainless steels) [53,54]. Thus, the anodic reaction reaches a limiting rate). The open circuit potential becomes higher under the passivation than that on a bare surface.

As seen from the above analysis based on electrochemical theory, the potential can increase under scaling conditions only if the anodic reactions are reduced more than the cathodic ones with the most plausible reason for this being when the actively corroding steel surface becomes passivated. However, there is no literature reporting this type of potential increase in steel immersion experiments in CO_2 environments. There are a few short term passivation studies which used potentiodynamic polarization to form passive film [28,29,34]. Clearly spontanous passivation achieved by immersion is more realistic than that through an artificial polarization, even if the two may lead to a similar outcome. Therefore the objective is now to clarify if the potential increase during scale formation on cathode of the galvanic cell is caused by passivation or by some other way. To achieve this goal, potentiodynamic polarization and cyclic polarization measurements were applied on bare and passivated surfaces. Spontaneously passivated surfaces prepared by immersion without external electrochemical stimuli were investigated.

2. Experimental

2.1. Setup

A typical three-electrode glass cell was used for the electrochemical measurements (Fig. 2) which was composed of mild steel working electrode (WE), platinum counter electrode (CE) and saturated Ag/AgCl reference electrode (RE).
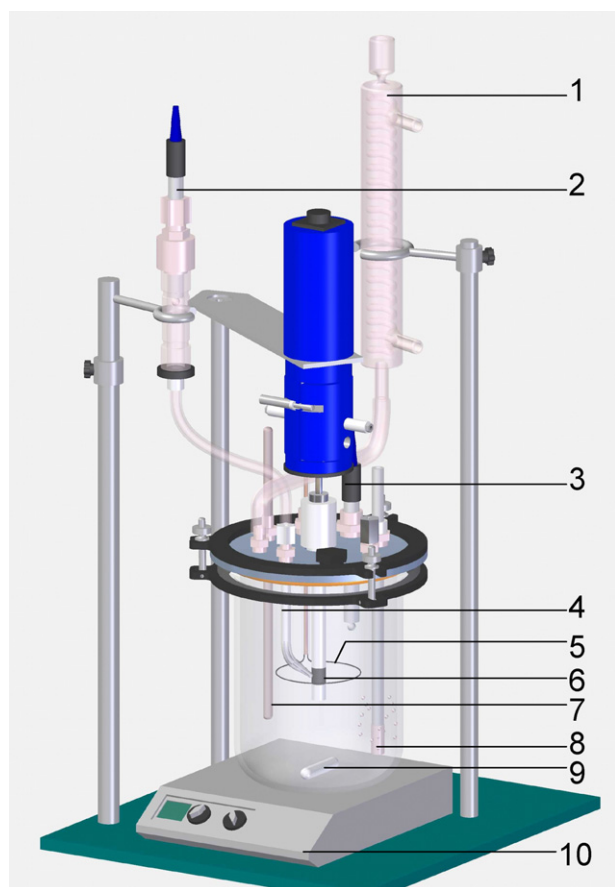
Fig. 2. Three electrode electrochemical glass cell arrangement. 1. – condenser, 2. – reference electrode, 3. – pH probe, 4. – Luggin capillary, 5. – platinum ring, 6. – working electrode, 7. – thermo probe, 8. – gas bubbler, 9. – magnetic stirrer bar, 10. – hotplate.

2.2. Procedures

Sodium chloride electrolyte (1 wt.% or 10 wt.%) was heated to the designated temperature and purged with carbon dioxide for at least 3 h. The pH was adjusted with solid $NaHCO_3$ (ACROS, ACS analytical grade 99.7%) 1 M solution and 0.1 M HCl. Extra deaeration was necessary to remove the dissolved oxygen during addition of $NaHCO_3$/HCl. The temperature was controlled automatically by the heating plate. The rotating cylindrical electrodes (RCE) were made of C1018 and X65 mild steel. They had an outer wall surface area 5.2 cm^2 and outer diameter 1.4 cm. The RCEs were polished sequentially by 240, 400, 600 grit sand paper, while cooled by flushing with 2-propanol during polishing, ultrasonicated in 2-propanol then blow dried. The electrodes were then immersed into the prepared electrolyte. The ferrous ion concentration was periodically measured. The pH was continuously monitored.

For the electrochemical measurements using potentiodynamic polarization, cathodic polarization started from stable open circuit potential. Anodic polarization was then executed only after a stable open circuit potential was reached again. Most of the specimens were polarized in less than 20 min after immersion at pH 7 and 8 to avoid any additional scale formation.

For the cyclic polarization, the polarization always began from the initial open circuit potential and increased in the positive direction and then reversed back to initial open circuit potential at scanning rates of 0.2 mV/s, 1 mV/s and 5.0 mV/s.

Spontaneous passivation was achieved when the open circuit potential increased and stabilized without any external electrochemical stimuli after the electrodes were immersed in the

Table 1
Material and test environments parameters.

RCE material	C1018, X65
RCE area/cm^2	5.4
RCE outer diameter/cm	1.4
RCE rotating speed (ω)/rpm	0, 300
Temperature/$°C$	25, 80
Partial pressure of CO_2/bar	0.97, 0.52
pH	7–9.5
NaCl concentration/(wt.%)	1, 10

Table 2
Parameters for electrochemical measurements.

Linear polarization resistance (LPR)	Polarization speed/(mV/s)	0.2
	Polarization range/(mV vs. OCP)	±5
Potentiodynamic polarization	Polarization speed/(mV/s)	0.2
	Anodic polarization range/(V vs. OCP)	0.6–0.8
	Cathodic polarization range/(V vs. OCP)	−0.2
Cyclic polarization	Polarization speed/(mV/s)	0.2, 1, 5
	Anodic polarization range/(V vs. OCP)	0.6–0.8
	Cathodic polarization range/(V vs. OCP)	−0.2

corrosion environment. Spontaneous passivation potential was in some cases 0.4 V higher than the open circuit potential for the fresh bare metal surface. Once spontaneous passivation was achieved, the electrochemical behavior of this passivated surface was investigated. This surface was then depassivated by reducing pH using deaerated 0.01 M hydrochloric acid in order to investigate the passive film damage/dissolution.

2.3. Test matrix

The test conditions and the parameter for electrochemical measurement are listed in Tables 1 and 2 respectively.

Environmental factors including NaCl concentration and pH were investigated. The salt concentration was adjusted to 1 wt.% and 10 wt.%. The pH was controlled at values between 7.0 and 8.0. For spontaneous passivation tests, the pH and temperature effects on spontaneous passivation were studied mainly in deaerated 1 wt.% NaCl electrolyte purged with CO_2 or N_2. In the depassivation tests, the temperature and initial pH were controlled at 80 °C and 7.8, respectively. Stepwise reduction in pH, used to initiate depassivation, was achieved by addition of hydrochloric acid with mild solution stirring in order to ensure good mixing.
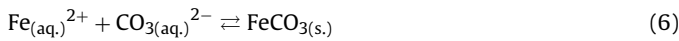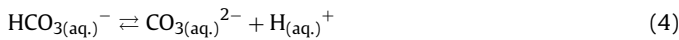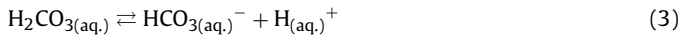
2.4. Sample analysis by TEM

Transmission electron microscopy (TEM) analysis was carried out using a FEI Tecnai F20 facility. A piece of cross-section surface was prepared by standard Focused Ion Beam (FIB) technique using ex-situ lift-out. The sample surface was first coated with gold to improve conductivity and then a thick layer of platinum was deposited on gold coating to both smooth the $FeCO_3$ surface and protect the cross-section during the FIB milling process. After thinning to electron transparency, the cross-sectional membrane was lifted out of the trench. It was then placed on a 20 nm carbon support film on a copper TEM grid to take image of steel-scale interface.
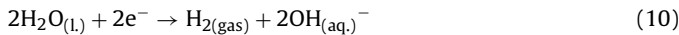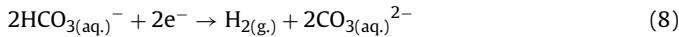
3. Results and discussion

In the CO_2 brine systems, key equilibria considered include dissolving, hydration and dissociation of CO_2, dissociation of water, and formation of iron carbonate. These equilibria are established by the following reactions [55]:

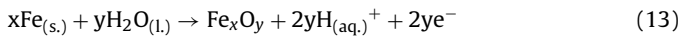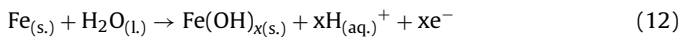$$CO_{2(gas)} \rightleftarrows CO_{2(aq.)} \tag{1}$$

$$CO_{2(aq.)} + H_2O \rightleftharpoons 2H_2CO_{3(aq.)} \tag{2}$$

$$H_2CO_{3(aq.)} \rightleftharpoons HCO_{3(aq.)}^- + H_{(aq.)}^+ \tag{3}$$

$$HCO_{3(aq.)}^- \rightleftharpoons CO_{3(aq.)}^{2-} + H_{(aq.)}^+ \tag{4}$$

$$H_2O_{(aq.)} \rightleftharpoons OH_{(aq.)}^- + H_{(aq.)}^+ \tag{5}$$

$$Fe_{(aq.)}^{2+} + CO_{3(aq.)}^{2-} \rightleftharpoons FeCO_{3(s.)} \tag{6}$$

On the steel surface, the electrochemical processes can be described by anodic (oxidation) and cathodic (reduction) half-cell reactions. The significant cathodic reactions are carbonic acid, bicarbonate, proton, and water reductions [56]:

$$2H_2CO_{3(aq.)} + 2e^- \rightarrow H_{2(g.)} + 2HCO_{3(aq.)}^- \tag{7}$$

$$2HCO_{3(aq.)}^- + 2e^- \rightarrow H_{2(g.)} + 2CO_{3(aq.)}^{2-} \tag{8}$$

$$2H_{(aq.)}^+ + 2e^- \rightarrow H_{2(gas)} \tag{9}$$

$$2H_2O_{(l.)} + 2e^- \rightarrow H_{2(gas)} + 2OH_{(aq.)}^- \tag{10}$$

The anodic reaction is the oxidative dissolution of iron [56]:

$$Fe_{(s.)} \rightarrow Fe_{(aq.)}^{2+} + 2e^- \tag{11}$$

When the surface is passivated, it is assumed that the iron oxidation reactions are to form iron hydroxides or iron oxides [54]:

$$Fe_{(s.)} + H_2O_{(l.)} \rightarrow Fe(OH)_{x(s.)} + xH_{(aq.)}^+ + xe^- \tag{12}$$

$$xFe_{(s.)} + yH_2O_{(l.)} \rightarrow Fe_xO_y + 2yH_{(aq.)}^+ + 2ye^- \tag{13}$$

3.1. Passivation observation using potentiodynamic polarization

3.1.1. Effect of pH on passivation

The potentiodynamic polarization was conducted on initially bare steel surface at pH 7 and pH 8 (Fig. 3). The initially active surface at pH 8 was passivated at a lower potential and current density. This indicates that passivation preferably occurs at a higher pH. A locally high pH can be achieved under an iron carbonate scale as demonstrated by Han et al. [49]. The local pH under an iron carbonate scale can be high enough (pH > 7 and pH < 9) to initiate passivation even if the bulk pH is acidic (e.g. pH 4–6). Many of the following tests were carried out under high pH, *ca.* 7–8, in order to speed up the scale formation by artificially creating the local alkalinity seen beneath the iron carbonate scale.

3.1.2. Effect of salt on passivation

Two potentiodynamic polarization were run at different salt concentrations to investigate its effect on passivation (Fig. 4). We observed lower pitting potential and higher pitting current density at higher Cl^- concentration of 10 wt.% salt. The current density was
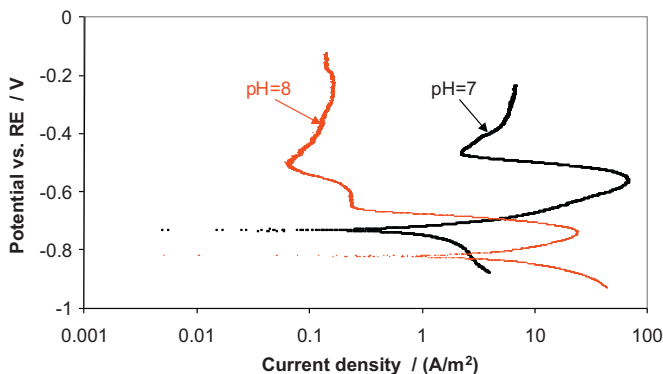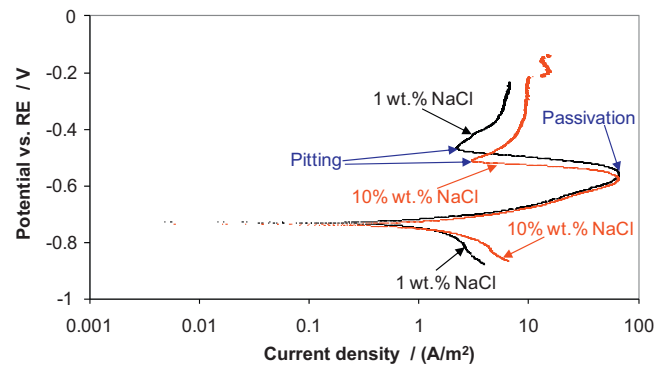

Fig. 4. Potentiodynamic polarizations applied from open circuit potential on bare surfaces at [NaCl] = 1 wt.%, 10 wt.%, pH = 7.0, $T = 80\,°C$, $P_{CO_2} = 0.53$ bar, $\omega = 0$ rpm.

higher at higher concentration of Cl^- anions for the same potential above the pitting potential. This is expected and it agrees with prevailing literature which suggests that Cl^- damages the passive film and accelerates localized corrosion [8]. The passivation potentials and passivation current densities at 1 wt.% and 10 wt.% NaCl concentrations were not significantly different. This is because a large amount of sodium bicarbonate (200 g) was also added to achieve solution pH of 7. The contribution to the ionic strength by NaCl (1 wt.%) was offset by the already present NaHCO_3 (20 wt.%). Therefore it is not surprising that the effect of NaCl on the passivation was masked by NaHCO_3.

3.1.3. Effect of FeCO_3 scale and passive film on polarization behavior

Mild steel can be passivated during immersion in CO_2 systems due to a passive film formation (this will be discussed in Section 3.3). After short term immersion, FeCO_3 scale was formed (at time indicated by in square A in Fig. 5). In longer immersions, a passive film was formed (less corrosion at higher potential), see square B in Fig. 5. Polarizations were carried out on initially bare, FeCO_3 scaled and passivated surfaces (Fig. 6). Comparing the polarization curves on bare and iron carbonate scaled surfaces, it was found that the anodic and cathodic current densities were reduced by the scale formation. The corrosion potential did not significantly vary during iron carbonate scale formation. This effect of iron carbonate scale was different from spontaneously passivated film. Firstly, the anodic and cathodic current densities on passivated surface were significantly retarded comparing to those on both bare and FeCO_3 scaled surfaces. Secondly, the open circuit potential was 0.4 V higher than that on bare and FeCO_3 scaled surfaces. These demonstrate typical passivation of the electrode, higher corrosion resistance at higher potential. Thirdly, surface passivation (as char-
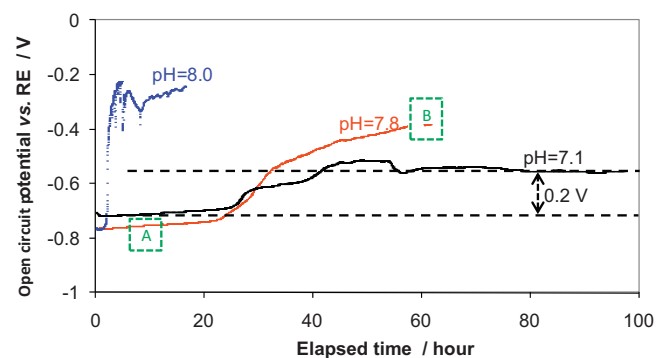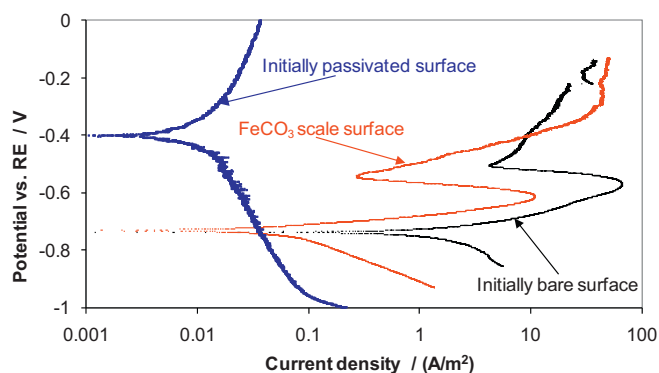

Fig. 3. Potentiodynamic polarizations applied from open circuit potential on bare surfaces at pH = 7.0, 8.0, [NaCl] = 1 wt.%, $T = 80\,°C$, $P_{CO_2} = 0.53$ bar, $\omega = 0$ rpm.

Fig. 5. The open circuit potential history during spontaneous passivation at pH = 7.1–8.0, $T = 80\,°C$, $P_{CO_2} = 0.53$ bar, [NaCl] = 1 wt.%, $\omega = 0$ rpm.

Fig. 6. Comparison of potentiodynamic polarizations from open circuit potential on bare, FeCO$_3$ scaled and spontaneously passivated surfaces at pH = 8.0, T = 80 °C, P$_{CO_2}$ = 0.53 bar, ω = 0 rpm.
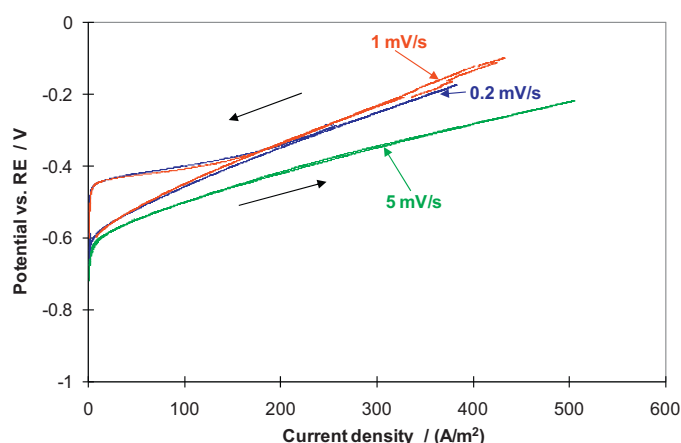
acterized by the inflection where the current density begins to decrease as the potential is forced to be more positive) did not show when comparing to polarizations on bare and FeCO$_3$ scaled surfaces. We can assume therefore that iron carbonate scale should not be the one which leads to passivation of the steel surface. Another chemical/phase is most likely be present to provide passivity of the steel and this will be investigated in the following Section 3.3.

3.2. Passivation observation from cyclic polarization

Cyclic polarization was applied to investigate the passivation behavior in a simulation of the local environment with the presence of iron carbonate scale at 80 °C and pH 8.0. The tests were run in dilute NaOH or NaHCO$_3$ solutions (for comparison) deaerated by nitrogen or carbon dioxide respectively.

Surface passivation was observed consistently in the CO$_2$ purged NaHCO$_3$ environments for all the cyclic polarization experiments (Fig. 7). The metal was passivated during the first half of the polarization sweep in which the potential was changed in the more positive direction. During the second half of each cyclic polarization, the potential was changed in the more negative direction following the end of the first half of the scan cycle. The passive film appeared to have survived during the reverse scan as evidenced by the lagged reduction peaks.

In the NaOH solution deaerated by nitrogen (without CO$_2$), passivation was only observed at the lower polarization rate of 0.2 mV/s and 1 mV/s (Fig. 8). The passivation potential was much higher than that at the same polarization rate in a CO$_2$ system with same bulk pH. This indicates that the passivation is more difficult to

Fig. 7. Cyclic polarizations applied starting from open circuit potential on mild steel at different scan rates in CO$_2$ purged NaHCO$_3$ electrolyte at T = 80 °C, pH = 8.0.

Fig. 8. Cyclic polarization applied starting from open circuit potential on mild steel at different polarization rates in N$_2$ deaerated NaOH electrolyte at T = 80 °C, pH = 8.0.

achieve under the alkaline solutions without the presence of either CO$_2$ or iron carbonate.

The observations through potentiodynamic and cyclic polarization support the assumption that mild steel passivation is preferably achieved at higher pH, *i.e.*, due to the locally increased pH beneath the iron carbonate scale.
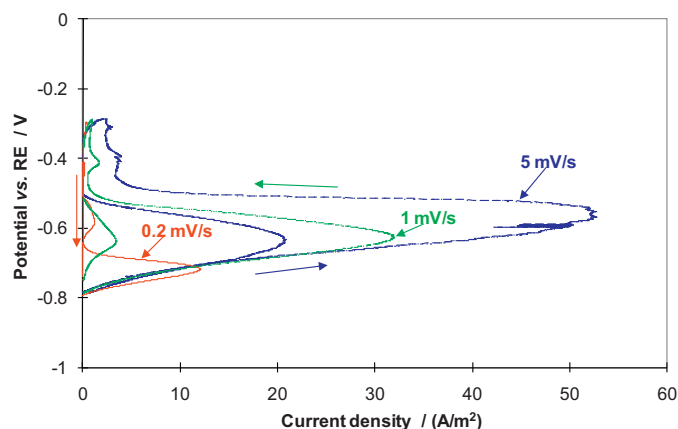
3.3. Spontaneous passivation observations

It has been clearly shown that the passivation of mild steel in CO$_2$ solutions can be achieved by anodic polarization, *i.e.*, by accelerating the anodic reaction. Therefore, new series of experiments were carried out to investigate if this would also happen spontaneously, in a process without any external electrochemical stimuli including any applied current or potential. This spontaneous passivation is a more realistic scenario closely related with the observations of localized corrosion and will be discussed in the following sections.
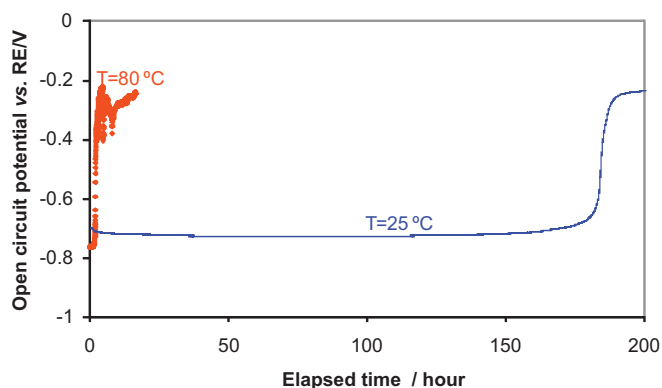
3.3.1. Effect of pH on spontaneous passivation

To carry out a spontaneous passivation test, fresh bare steel was immersed in the electrolyte with a pH range from 7.1 to 8.0 to corrode without external polarization, *i.e.*, at its open circuit potential. An open circuit potential increase was observed after a few hours of immersion (Fig. 5). The time to reach spontaneous passivation was longer at lower pH. This is not surprising as more time is required to accumulate sufficient ferrous iron to form a corrosion scale and a passive film. The stabilized spontaneous passivation potential tended to decrease at lower pH values.

These experiments can be seen as a direct proof of the hypothesis made at the beginning of this paper suggesting that spontaneous passivation will occur and increase the potential of the steel electrode. It is important to bear in mind what the implications of spontaneous passivation are for localized corrosion. Recall an experiment where carbon steel has been completely spontaneously passivated at a pH of 7.1 (Fig. 5). The open circuit potential is around −0.55 V vs. RE. If the iron carbonate scale and the passive film are partially damaged, the open circuit potential for the bare metal surface would be equal to −0.73 V vs. RE. A galvanic cell would be established between these two surfaces. The potential difference (*ca.* 0.2 V) can, in theory, cause localized corrosion rates to be thousands of times greater than the uniform corrosion rate of a bare metal surface. These extreme numbers were estimated without consideration of IR drop, mass transfer and pit geometry.

Fig. 9. The open circuit potential history during spontaneous passivation at $T = 25\,°C$, $80\,°C$, pH = 8.0, $P_{CO_2} = 0.53$ bar, NaCl = 1 wt.%, $\omega = 0$ rpm.

3.3.2. Effect of temperature on spontaneous passivation

The spontaneous passivation experiments carried out at different temperature, 25 °C and 80 °C showed that the time to reach spontaneous passivation was longer at lower temperatures (Fig. 9). This is expected that the kinetics is accelerated at high temperature. No significant difference was observed for spontaneous passivation potential.

3.3.3. Effect of $CO_2/FeCO_3$ on the spontaneous passivation

From the potentiodynamic polarization experiments, preliminary results suggested that CO_2, most probably $FeCO_3$, was necessary to assist in the passivation of the steel. Its effect on the spontaneous passivation was investigated in the following series of experiments. The passivation tests were carried out at 80 °C and pH 8 and 9.5 in electrolyte of NaCl, NaOH and $NaHCO_3$ saturated with CO_2, N_2 and their mixture.

The spontaneous passivation test results showed that spontaneous passivation was observed even with a 7% molar fraction of CO_2 in the gas phase, but was not observed when pure N_2 was used as the purge gas (Fig. 10).

A possible reason for the lack of spontaneous passivation in the absence of CO_2 could be that the corrosion rate is different for these two systems although they were under the same pH. This is due to extra cathodic reactions, carbonic acid and bicarbonate reduction, which leads to a much higher corrosion rate in a CO_2 system comparing to a N_2 system, and generates a higher concentration of ferrous ion required for scaling and passivation. As measured, the corrosion rate under the CO_2 purged solution can reach 2–3 mm/year [56], which was one magnitude lower than the
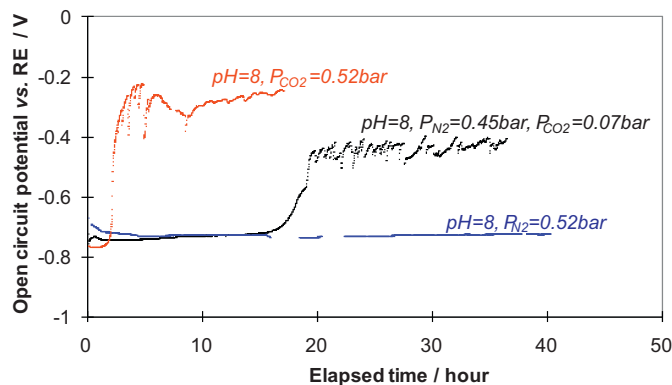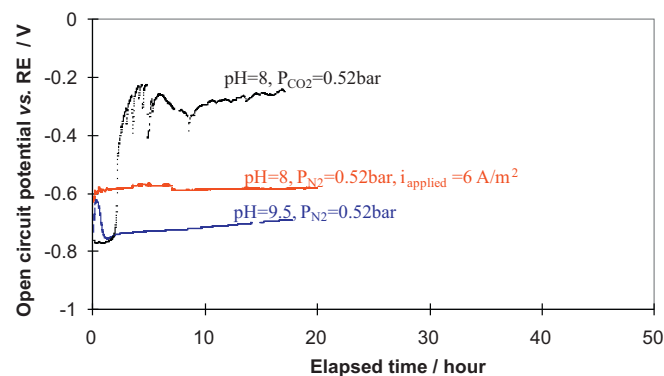
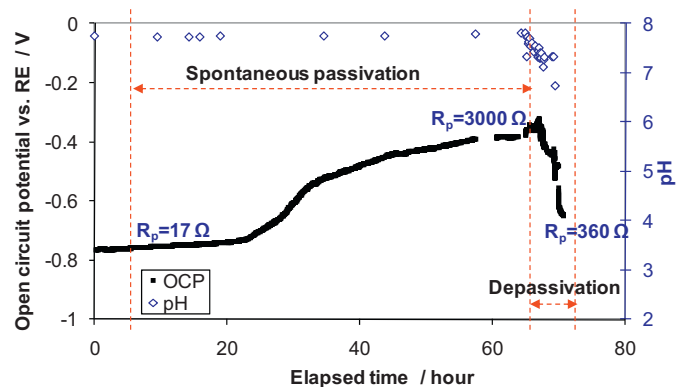

Fig. 11. The open circuit potential history during spontaneous passivation of mild steel in nitrogen deaerated NaOH solution comparing to CO_2 purged solution at pH = 8.0, 9.5, $P_{N_2} = 0.52$ bar, $P_{CO_2} = 0.52$ bar, or applied anodic current density = 6 A/m².

corrosion rate under N_2 purged electrolyte. In an attempt to prove this hypothesis, an anodic current was applied to the steel sample in N_2 purged solution, which resulted in a corrosion rate almost three times higher than that in the CO_2 saturated electrolytes. However, the hypothesis had to be discarded as spontaneous passivation was not achieved (Fig. 11). The steel surface was not spontaneously passivated even at a pH of 9.5 in the nitrogen purged NaOH solution. Thus, this argument suggests that formation of passive films is closely related with the presence of $CO_2/FeCO_3$.

3.3.4. Roles of $FeCO_3$ on passivation and depassivation

From the above discussion on the role of iron carbonate scale in passivation, it appears that $FeCO_3$ scale promotes mild steel passivation. We can go one step further and boldly assume that the passive film is made up of iron carbonate. One can then assume that passivation can only be achieved when the saturation point for iron carbonate is greater than unity and should dissolve away if the solution becomes undersaturated with respect to iron carbonate. The first part of this hypothesis was proven many times and described in the text above. However, the second half of the hypothesis requires further investigation by inducing depassivation by decreasing pH where an iron carbonate scale already formed and passivation was observed.

A typical potential profile in a spontaneous passivation and depassivation test called "Case 1", is depicted in Fig. 12. This case shows that after passivation was achieved, depassivation was directly related to the pH decrease as indicated by the decrease in open circuit potential. A more detailed version of the same graph

Fig. 10. The open circuit potential history during spontaneous passivation of mild steel in nitrogen deaerated NaOH solution comparing to CO_2 purged solution at $T = 80\,°C$, pH = 8.0, $P_{N_2} = 0.45$ bar, 0.52 bar, $P_{CO_2} = 0.07$ bar, 0.52 bar.

Fig. 12. Case 1: the spontaneous passivation at initial pH = 7.8, $T = 80\,°C$, $P_{CO_2} = 0.53$ bar, [NaCl] = 1 wt.%, $\omega = 0$ rpm and depassivation by decreasing pH from pH 7.8 to pH 5.4.
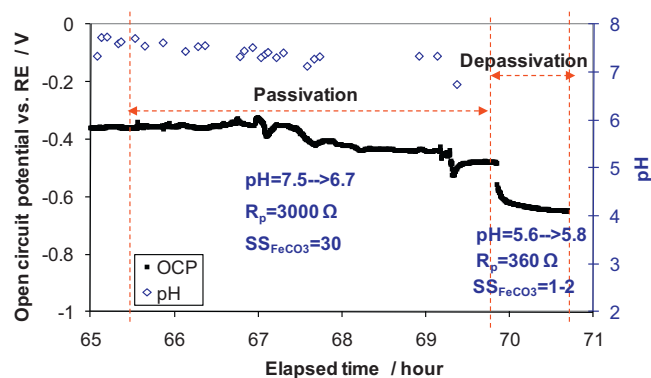
Fig. 13. Case 1: potential history during depassivation by reducing pH from 7.5 to 5.6 at $T = 80\,°C$, $P_{CO_2} = 0.53$ bar, [NaCl] = 1 wt.%, $\omega = 300$ rpm.
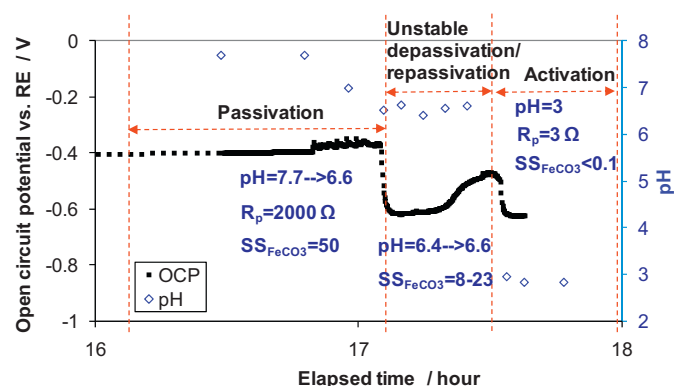
Fig. 14. Case 2: potential history during depassivation by reducing pH from 7.7 to 3.0 at $T = 80\,°C$, $P_{CO_2} = 0.53$ bar, [NaCl] = 1 wt.%, $\omega = 300$ rpm.

with passivation/depassivation region is given in Fig. 13 where values for pH and $FeCO_3$ supersaturation calculated from the model by Han et al. [56], were added, both of which directly related to $FeCO_3$ formation/dissolution. Note that during depassivation, the solution conditions with respect to $FeCO_3$ actually remained supersaturated (saturation $\gg 1$) as the pH was decreased and passivation was gradually lost. This implies that the ferrous carbonate scale did not dissolve, but the mild steel surface depassivated. The survival of iron carbonate scale was confirmed by the larger polarization resistance comparing to that of bare surface.

Attention must be drawn to the fact that the polarization resistance increased from $17\,\Omega$ for the bare surface to $3000\,\Omega$ for the passivated surface. After the depassivation, the passive film was lost while iron carbonate scale remained intact. The polarization resistance became $360\,\Omega$. This observation indicates that protective iron carbonate scale can retard corrosion kinetics somewhat but also demonstrates the super-protectivity of the passive film.

It can be argued that in the previous experiment iron carbonate was near the saturation point and could have dissolved due to slight fluctuations in solution conditions or an error in our ability to predict saturation conditions accurately. To check this possibility, another previously scaled and passivated surface was then depassivated by carefully and slowly decreasing the pH as depicted in Fig. 14 (called Case 2). In this experiment, the steel surface lost passivation in the pH range of 6.4–6.6. The subsequent repassivation in the same range of pH clearly suggests this range should be considered the initiation point of the passivation while the calculation of iron carbonate supersaturation of $SS_{FeCO_3} = 8$–23 shows the bulk solution supersaturation value is well above unity. For this condition, iron carbonate formed should remain in place.

In summary, all the depassivation experimental results clearly confirmed that passivation occurs only after iron carbonate scale was formed. However, depassivation can happen with this $FeCO_3$ scale intact, i.e., while the bulk solution is still supersaturated. This agrees indirectly with passive layer composition containign other compounds such as magnetite or iron hydroxides as reported by Han et al. [24].

### 3.4. TEM analysis of spontaneously passivated scale-steel interface

In the high-angle annular dark-field TEM image of the cross-sectional sample after spontaneous passivation (Fig. 15), the brighter areas corresponds to increased scattering of the electrons by a phase with higher averaged atomic weight. At the top of the sample are the platinum protective layer and the gold conductive coating. The interface between the iron and the iron carbonate appeared rougher at the steel grain boundaries. At the iron carbonate crystal grai boundary, an extra phase (grey color), ca. 140 nm thick, was observed (Fig. 16). At the bottom of the iron carbonate crystal, only a 12 nm grey phase was observed (as shown in Fig. 17). Bearing in mind that the iron carbonate phase is darker than the iron substrate because it has a lower average atomic number the grey phase's color weight being in between $FeCO_3$ and Fe indicates that chemical in the extra phase has an averaged atom weight between $FeCO_3$ and Fe. The iron hydroxides are not possiblity since their average atom weights are less than $FeCO_3$: $Fe(OH)_2$ is 18 and $Fe(OH)_3$ is 15. The likely chemicals are iron oxides: FeO is 36, Fe_3O_4 is 33 and Fe_2O_3 is 32. FeO is not a stable corrosion
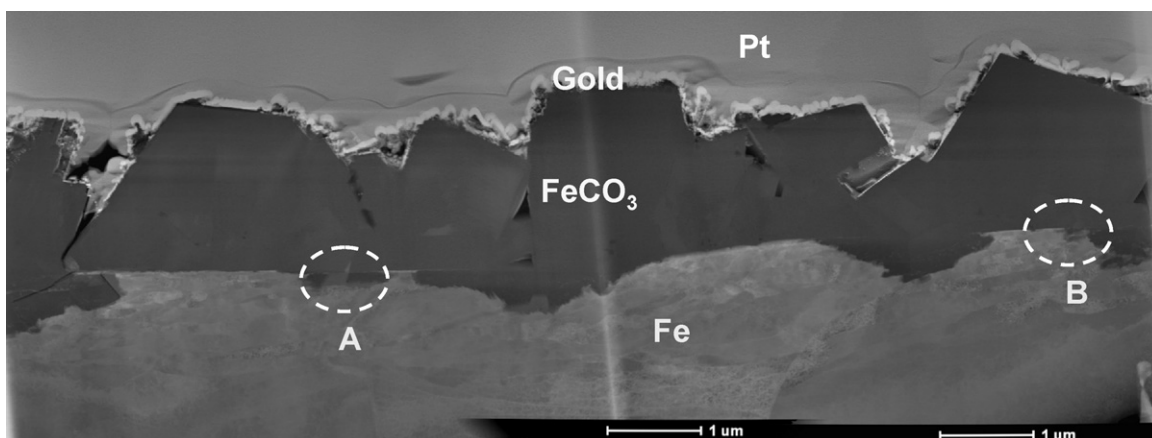
Fig. 15. The TEM image of a slice of cross section sample by FIB taken from the bulk surface passivated at pH 8.0, $T = 80\,°C$, NaCl = 1wt%, $P_{CO_2} = 0.53$ bar, $\omega = 0$, rpm.
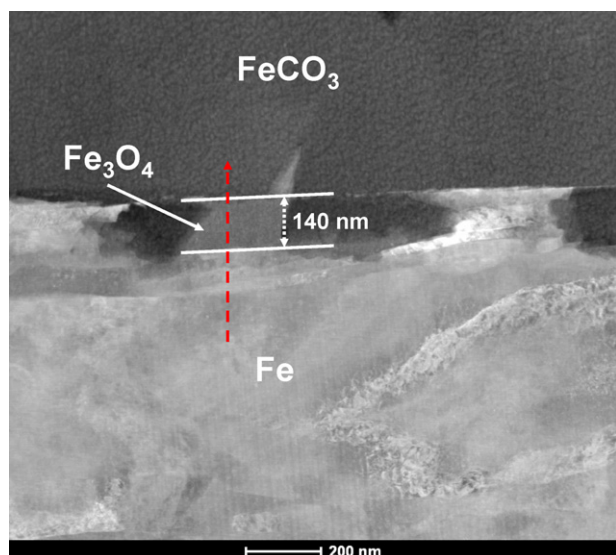
Fig. 16. The TEM image of steel-scale interface at the iron carbonate crystal edge (area A in Fig. 15).
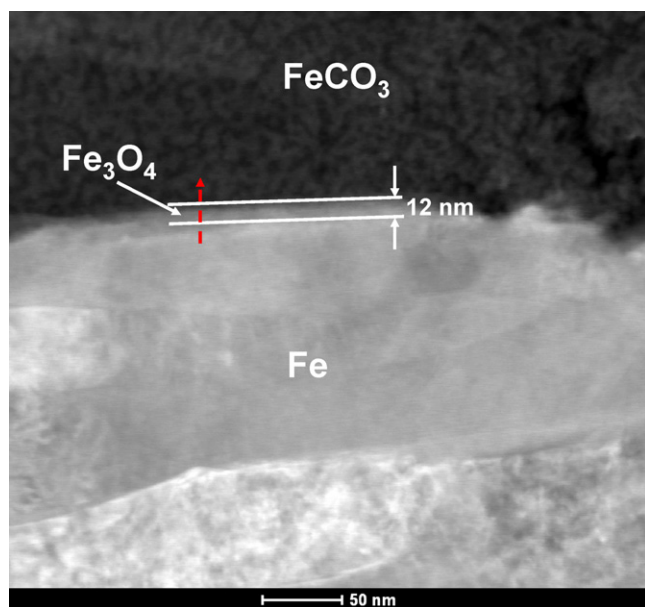
Fig. 17. TEM image of steel-scale interface at the iron carbonate crystal bottom (area B in Fig. 15).

product in CO_2 system. Fe_2O_3 is less likely formed in reductive CO_2 environment. The most possible chemistry of the passive phase is Fe_3O_4. This conclusion agrees with the literature results where the passive film chemistry and structure were measured by TEM/EDX combining grazing incidence x-ray diffraction [24].

4. Conclusions

Passivation of mild steel in CO_2 solutions has been investigated using potentiodynamic polarization and cyclic polarization techniques. From potentiodynamic polarization tests, the observation of lower passivation potential and current density at high pH indicated that passivation was achieved preferably in a alkaline environment, such as the local environment formed underneath iron carbonate scale. The presence of iron carbonate scale promoted passivation to occur at a lower potential and current density. Cyclic

polarization tests show that a high polarization rate increased the passivation potential and current density.

Spontaneous passivation, a state of high corrosion resistance at higher potential, was observed through immersion tests without any externally applied current or potential. Spontaneous passivation was favorably achieved at high pH, high temperature and with the presence of aqueous $CO_2/FeCO_3$. Nevertheless, iron carbonate scale was not the film responsible for passivation. This was clearly demonstrated when passivity was lost without losing the existing iron carbonate scale and that iron carbonate can be formed without increasing the potential.

The steel-scale interface was analyzed by TEM. An extra phase between iron carbonate and iron was observed. The averaged atom weight was between that of iron and iron carbonate. This phase is most possibly magnetite.

The mild steel may spontaneously passivate in higher pH environments which results in increased potential. If the protective layer gets removed mechanically or chemically, the presence of a bare surface due to local damage of passive film allows the establishment of a galvanic cell. The potential difference between these two surfaces drives accelerated corrosion on bare steel surface, leading to localized corrosion.

References

[1] Y.P. Virmani, Corrosion cost and preventive strategies in the United States, report no. FHWARD-01-156, 2002.
[2] D.C. Eden, D.A. Eden, R.D. Kane, Innovative corrosion monitoring solutions enhance process optimization, http://www.chemicalprocessing.com/articles/2005/525.html (accessed April 6, 2010).
[3] U.R. Evans, A.C. Hart, J. Chem. Soc. (1930) 478.
[4] T.E. Evans, A.C. Hart, Electrochim. Acta 16 (1971) 1955.
[5] N. Sato, K. Kudo, Electrochim. Acta 16 (1971) 447.
[6] B.E. Conway, M.A. Sattar, D. Gilroy, Electrochim. Acta 14 (1969) 677.
[7] C.J. Chatfield, L.L. Shreir, Electrochim. Acta 14 (1969) 1015.
[8] H.S. Srinivansan, C.K. Mital, Electrochim. Acta 39 (1994) 2633.
[9] X.L. Shang, B. Zhang, E.H. Han, W. Ke, Electrochim. Acta 56 (2011) 1417.
[10] J.O. Zerbino, L.M. Gassa, J. Solid State Electrochem. 7 (2003) 177.
[11] G.R. Engelhard, L.G. McMillion, D.D. Macdonald, J. Nucl. Mater. 379 (2008) 48.
[12] J.N. Harb, R.C. Alkire, Corros. Sci. 29 (1989) 3143.
[13] A. Machet, A. Galtayries, S. Zanna, L. Klein, V. Maurice, P. Jolivet, M. Foucault, P. Combradec, P. Scott, P. Marcus, Electrochim. Acta 49 (2004) 3957.
[14] G.S. Frankel, J. Electrochem. Soc. 145 (1998) 2186.
[15] W. Zhang, G.S. Frankel, Electrochim. Acta 48 (2003) 1193.
[16] G.S. Frankel, M. Stratmann, M. Rohwerder, A. Michalik, B. Maier, J. Dora, M. Wicinski, Corros. Sci. 49 (2007) 2021.
[17] G.S. Frankel, N. Sridhar, Mater. Today 11 (2008) 38.
[18] D.D. Macdonald, B. Oberts, Electrochim. Acta 23 (1978) 557.
[19] D.D. Macdonald, M. Urquidi-Macdonald, J. Electrochem. Soc. 137 (1990) 2395.
[20] D.D. Macdonald, J. Electrochem. Soc. 139 (1992) 3434.
[21] J.C. Walton, Corros. Sci. 30 (1990) 915.
[22] S.M. Sharland, Corros. Sci. 27 (1987) 289.
[23] J. Kruger, in: R.W. Revie (Ed.), Uhlig's Corrosion Handbook, 2nd ed., John Wiley & Sons Inc., New York, 2000, Ch. 9.
[24] J. Han, D. Young, H. Colijn, A. Tripathi, S. Nešić, Ind. Eng. Chem. Res. 48 (2009) 6296.
[25] C. deWaard, D.E. Williams, Corrosion 31 (1975) 177.
[26] C.R.F. Azevedo, Eng. Fail. Anal. 14 (2007) 978.
[27] S.D. Zhu, J.F. Wei, Z.Q. Bai, G.S. Zhou, J. Miao, R. Cai, Eng. Fail. Anal. (2010), doi:10.1016/j.engfailanal.2010.11.013.
[28] A Wieckowski, E. Ghali, M. Szklarczyk, J. Sobkowski, Electrochim. Acta 28 (1983) 1619.
[29] A. Wieckowski, E. Ghali, M. Szklarczyk, J. Sobkowski, Electrochim. Acta 28 (1983) 1627.

[30] K. Videm, A. Dugstad, Mater. Performance (1989) 63.
[31] K. Videm, A. Dugstad, Mater. Performance (1989) 46.
[32] M.W. Joosten, T. Johnsen, H.H. Hardy, J. Jossang, J. Feder, NACE CORROSION conf., paper no. 406, 1992.
[33] M.W. Joosten, T. Johnsen, A. Dugstad, T. Walmann, J. Jossang, P. Meakin, J. Feder, NACE CORROSION conf., paper no. 3, 1994.
[34] K. Videm, A.M. Koren, NACE CORROSION conf., paper no. 12, 1992.
[35] A. Marie, K. Halvorsen, T. Søntvedt, NACE CORROSION conf., paper no. 42, 1999.
[36] M.H. Achour, J. Kolts, A.H. Johannes, G. Liu, NACE CORROSION conf., paper no. 87, 1993.
[37] G. Schmitt, W. Bucken, R. Fanebust, Corrosion 48 (1991) 431.
[38] C.F. Chen, M.X. Lu, D.B. Sun, Z.H. Zhang, W. Chang, Corrosion 61 (2005) 594.
[39] Z. Xia, K.C. Chou, Z. Szklarska-Smialowska, Corrosion 45 (1989) 636.
[40] J.L. Crolet, in: B. Kermani (Ed.), Predicting CO_2 Corrosion in the Oil and Gas Industry, European Federation of Corrosion Publications, London, 1994, no. 13.
[41] R. Nyborg, A. Dugstad, NACE CORROSION conf., paper no. 642, 2003.
[42] J. Amri, E. Gulbrandsen, R.P. Nogueira, Electrochem. Commun. 10 (2008) 200.
[43] J. Amri, E. Gulbrandsen, R.P. Nogueira, Electrochim. Acta 54 (2009) 7338.
[44] G.A. Zhang, Y.F. Cheng, Electrochim. Acta 56 (2011) 1676.
[45] J. Han, Y. Yang, B.N. Brown, S. Nešić, NACE CORROSION conf., paper no. 07323, 2007.
[46] J. Han, Y. Yang, B.N. Brown, S. Nešić, NACE CORROSION conf., paper no. 08332, 2008.
[47] J. Han, D. Young, S. Nešić, A. Tripathi, ICC conf. paper no. 2511, 2008.
[48] J. Han, S. Nešić, B.N. Brown, ICC conf., paper No. 2687, 2008.
[49] J. Han, B.N. Brown, D. Young, S. Nešić, J. Appl. Electrochem. 40, 683, 2010.
[50] J. Han, B.N. Brown, S. Nešić, Corrosion 66, 095003 1, 2010.
[51] Y. Tan, Y.F. Wu, K. Bhardwaj, S. Bailey, R. Gubner, NACE CORROSION conf., paper no. 10155, 2010.
[52] K. Lepková, R. Gubner, NACE CORROSION conf., paper no. 10331, 2010.
[53] D.A. Jones, Principles and Prevention of Corrosion, 2nd ed., Prentice Hall, Inc., Upper Saddle River, NJ, 1996.
[54] B. MacDougall, M.J. Graham, in: Philippe Marcus (Ed.), Corrosion Mechanisms in Theory and Practice, 2nd ed., Marcel Dekker Inc., New York, 2002, Ch. 6.
[55] D.A. Palmer, R. Van Eldik, Chem. Rev. 83 (1983) 651.
[56] J. Han, J.W. Carey, J. Zhang, Int. J. Greenh. Gas Cont. 5 (2011), doi:10.1016/j.ijggc.2011.02.005.